Sc Modification Induced Short-range Ordering in ZnGa2O4 Spinel Leading to High Microwave Dielectric Performance

xiaochi Lu
College of Electronic and Optical Engineering & College of Microelectronics, Nanjing University of Posts and Telecommunications, Nanjing 210023, P.R. China https://orcid.org/0000-0003-3651-6167

Bin Quan
Nanjing University of Information Science and Technology

Kailai Zheng
Nanjing University of Posts and Telecommunications

Peng Chu
Nanjing University of Posts and Telecommunications

Jian Wang
Nanjing University of Posts and Telecommunications

Guangxu Shen
Nanjing University of Posts and Telecommunications

Qitu Zhang
Nanjing Tech university

Feng Xu (feng.xu@njupt.edu.cn)
College of Electronic and Optical Engineering & College of Microelectronics, Nanjing University of Posts and Telecommunications, Nanjing 210023, P.R. China

Research Article

Keywords: ZnGa2O4, spinel, Sc3+ modification, bond vibration, microwave dielectric materials

Posted Date: October 30th, 2020

DOI: https://doi.org/10.21203/rs.3.rs-98833/v1

Sc modification induced short-range ordering in $ZnGa_2O_4$ spinel leading to high microwave dielectric performance

Xiaochi Lu[a], Bin Quan[b], Kailai Zheng[a,d], Peng Chu[a], Jian Wang [a], Guangxu Shen[a], Qitu Zhang[c], Feng Xu[a,*]

a College of Electronic and Optical Engineering & College of Microelectronics, Nanjing University of Posts and Telecommunications, Nanjing 210023, P.R. China
b Institute of Advanced Materials and Flexible Electronics (IAMFE), School of Chemistry and Materials Science, Nanjing University of Information Science & Technology, Nanjing 210044, P.R. China
c College of Materials Science and Engineering, Nanjing Tech University, Nanjing, 210009, P. R. China.
d State Key Lab. of Millimeter Waves, Southeast University, Nanjing 210096, P.R. China
* Corresponding Author, Prof. Feng Xu E-mail: feng.xu@njupt.edu.cn

Abstract

Sc^{3+} (0,0.1,0.3,0.5,0.7mol%) modified $ZnGa_2O_4$ (abbreviated Sc-ZGO) ceramics were synthesized by solid-state method. The relationship between microwave dielectric performance and bonds vibration of Sc-ZGO as a function of Sc^{3+} modification has been systematically investigated. With Sc^{3+} modification, the ε_r of Sc-ZGO ceramics keeps steady (~10). While the τ_f of Sc-ZGO shows linear correlation with Sc^{3+} concentration increasing from -71ppm/°C to -39ppm/°C, and the $Q\times f$ value climbs up to a maximum value (5Sc-ZGO) and then ramp down. 5Sc-ZGO sintered at 1350°C for 2 h exhibits the best microwave dielectric properties with ε_r = 9.9, $Q\times f$ = 124,147 GHz, tanδ = 7.98×10^{-5}, and τ_f = -56 ppm/°C (@9.9 GHz). $Q\times f$ value of Sc modified ZGO increased by almost 45% compared with normal spinel $ZnGa_2O_4$ ceramics. The enhancement of τ_f and $Q\times f$ on Sc modified $ZnGa_2O_4$ can be attributed to higher densification, however, further Raman and FT-IR analysis elucidated that short-range cation ordering degree is another governing factor. The influence of Sc^{3+} modification on $ZnGa_2O_4$ bonds vibration has been discussed in detail.

Keywords

$ZnGa_2O_4$; spinel; Sc^{3+} modification; bond vibration; microwave dielectric materials

Introduction

Spinel-type compounds AB_2O_4 have been extremely investigated in science and technical fields such as phosphor [1-2], catalysts [3-4], semiconductors [5-6], superconductors [7-8] and microwave dielectric materials [9-12]. Among these applications, microwave dielectric materials in high frequency (5G) is one of the most important applications with wide investigations. The framework of Spinel-type compounds has close packed tetrahedral (AO_4 or BO_4) and octahedral (BO_6 or AO_6). This type of crystal structure has a great variability because of variety cation selections,

and possibilities in cation ordering such as common spinel (AB_2O_4), inverse spinel ($B(AB)O_4$) and mixed-type spinel. So far, spinel structured ceramics for high frequency application include M_2SnO_4 [13-14], M_2SiO_4 [15-16], MAl_2O_4 (M=Zn, Mg) [17-18] and MGa_2O_4 (M = Zn, Mg) [19-23].

However, the development and application of stannate are limited by large negative τ_f and low $Q\times f$. As for silicate, it is difficult to prepare because of their sensitivity to synthesis conditions. Although the quality factor of aluminate can exceed 60,000 GHz, its sintering temperature is relatively high as well as silicate. Cause most of the spinel ceramics need high sintering temperature for about 1600°C. Considering environment friendly materials, explorations in lower sintering temperature by materials design and composition engineering are increased. Compared with M_2SnO_4, M_2SiO_4 and MAl_2O_4 (M=Zn, Mg), MGa_2O_4 have good microwave dielectric properties, lower sintering temperature and a wide sintering temperature region. Therefore, MGa_2O_4 (M=Zn,Mg) materials are promising candidates for high frequency (5G) applications.

For MGa_2O_4 (M=Zn, Mg) materials, $ZnGa_2O_4$ is a normal spinel and $MgGa_2O_4$ is a mixed-type spinel. Thus, the crystal structure of $MgGa_2O_4$ is more complexed than the former one and the mixed proportion varied with synthesis conditions which brings more difficulties to reveal relationships among synthesis conditions, modification, crystal structure and microwave dielectric properties. Hence, $ZnGa_2O_4$ with normal spinel structure got our attention. It is reported that $ZnGa_2O_4$ possesses lower sintering temperature (1400°C), large sintering range (1300°C -1500°C) with excellent dielectric performance (ε_r = 9.8, $Q\times f$ = 83,000 GHz, τ_f = -71 ppm/°C) [10]. However, relatively large negative τ_f (-71 ppm/°C), and the relatively large tanδ (19×10^{-5}) are the two difficulties in the application of $ZnGa_2O_4$ microwave dielectric ceramics.

For microwave dielectric materials possessing high density and good crystallinity, the initial temperature coefficient at resonant frequency (τ_f) can be got through formula 1 as follows [24]:

$$\tau_f = -(\frac{1}{2}\tau_\varepsilon + \frac{1}{2}\tau_\mu + \alpha_L) \quad (1)$$

Thus, the permittivity coefficient (τ_ε), permeability coefficient (τ_μ), coefficient of thermal expansion (α_L) are three considerable factors to influence the τ_f. That means adjusting τ_ε, τ_μ, and α_L can obtain near zero τ_f. In our previous study, TiO_2 was applied to form TiO_2-$ZnGa_2O_4$ composite ceramics to adjust τ_ε and through this method near zero τ_f was obtained at $0.1TiO_2$-$0.9ZnGa_2O_4$ [19]. Another study applied Mn to modified the τ_μ of $ZnGa_2O_4$ and it successfully shift τ_f from -71ppm/°C to -12ppm/ °C [20].

To achieve a high signal noise ratio to ensure transmission quality, resonators should possess higher $Q\times f$. $1/Q$ is the total loss (tanδ) and can be figured out through formula 2 [25] . $1/Q_d$, $1/Q_c$, $1/Q_r$, and $1/Q_{ext}$ are related to dielectric, conductor, radiation and external power loss, respectively.

$$\frac{1}{Q} = \frac{1}{Q_d} + \frac{1}{Q_c} + \frac{1}{Q_r} + \frac{1}{Q_{ext}} \quad (2)$$

Classically, materials with close packed, ordered structure, high density, good crystallinity and fine morphology possess low dielectric loss because of lower vibration

loss, grain boundary and impurity loss. In our previous study, Cr^{3+} doped $ZnGa_2O_4$ obtain excellent microwave dielectric properties due to the higher density and higher short-range cation ordering [21]. Cu^{2+} was also applied to form Cu-ZGO solid solutions and obtain mixed spinel structure, the higher density and higher short-range cation ordering contribute to the higher $Q \times f$ [22-23].

Rare earth (RE) elements possess special atomic structure, physical and chemical properties which is mainly caused by their 4f electron configuration. The special structure of RE elements which leads to special optical, electrical, magnetic and thermal properties. And the application of RE elements in many ceramic materials has made great progress. Thus, RE modification have been applied extensively to control microstructures, crystal structures and dielectric properties, especially in piezoelectric ceramics and microwave dielectric ceramics like PZT [26], Ca/BaO-Ln_2O_3-TiO_2 [27] and CaO-Ln_2O_3-TiO_2-Li_2O [28]. The most used RE elements are Nd, Y, Sm and Ce, however, Sc has not yet been studied in this respect.

Based on the above discussion, Sc modified $ZnGa_2O_4$ (abbreviated Sc-ZGO) were designed to achieve higher $Q \times f$ and near zero τ_f. As a result, we obtain a low ε_r of 10 at 13GHz, sintered at 1350°C for 2 h which is lower than most of spinel ceramics without sintering additives. The microwave dielectric performance of Sc-ZGO, demonstrating low dielectric loss, and a near zero τ_f was achieved. Thus, it can provide guidance on the enhancement of spinel-type microwave dielectric ceramics properties.

Materials and Methods

Sample preparation

Solid state reactions were adopted to prepare Sc-ZGO with Sc content range from 0.1mol to 0.7mol%, using analytical grade Sc_2O_3, Ga_2O_3, and ZnO. According to the Sc-ZGO chemical formula, Sc_2O_3, Ga_2O_3, and ZnO were weighted and ball milled in polyethylene jars for one day with ethanol. These mixtures were dried at 80°C for one day and then calcined at 1000°C for 2 h. The green ceramics pellets with diameter~13 mm and thickness ~6 mm, was obtained under an uniaxial pressure ~75 MPa for 1min, and then sintered at 1300-1450 °C for 4 h in high-temperature electric furnace (KSX4-16, Allfine, Wuxi, China).

Characterization

The micromorphology of Sc-ZGO was detected by a scanning electron microscope (SEM) (Hitachi SU8010, Japan). Archimedes' method was applied to measure the density of the given samples. Phase composition and evolution of Sc modified $ZnGa_2O_4$ ceramics were identified via X-ray diffraction (XRD) (Rigaku Cu, RigakuD/Max 2500, Japan) and Raman spectroscopy (Raman) (HR800, Horiba Labram, 514 nm He-Cd laser, 20mW laser power). The high resolution TEM (HRTEM) images and selected-area electron diffraction (SAED) patterns were achieved at 200 kV using a transmission electron microscope (JEM-2100, JEOL). X-ray photoelectron spectrometer (XPS) (ESCALAB 250, Thermo Fisher, UK) was employed to collect XPS data to reveal elements chemical status in Sc-ZGO and the X-ray source was Al-Kα. Microwave dielectric performance, including ε_r, tanδ, f and τ_f, were measured using the cavity

resonator method [29] via a Lightwave Component Analyzer (Hewlett Packard 8703A, 1550 nm/130 MHz to 20 GHz). A NICOLET 5700 FT-IR spectrometer (Thermo, America) were applied to get the Fourier transform infrared (FT-IR) spectrum.

Results and Discussion

Microstructure of Sc-ZGO ceramics

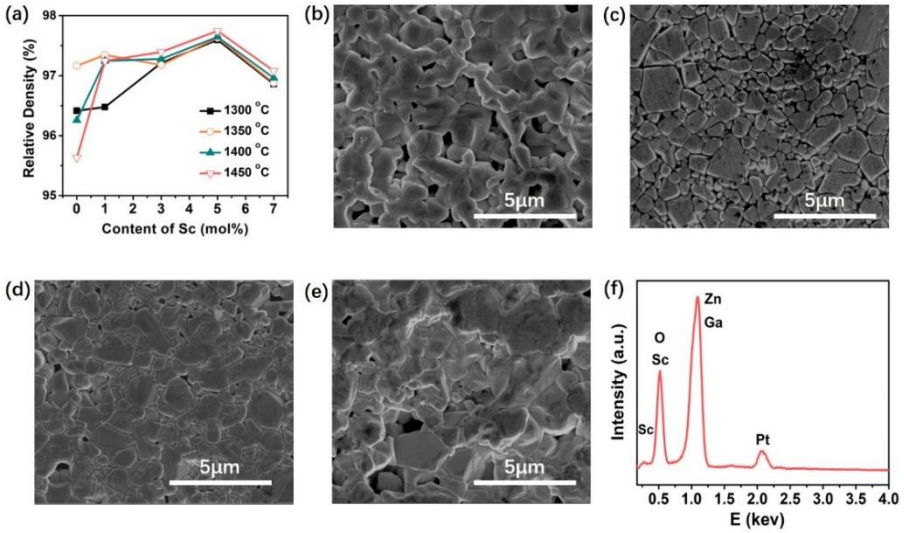

Fig. 1 (a) Relative density of Sc-ZGO, SEM images of Sc-ZGO sintered at 1350 ºC for 2 h and (b-e) are 1Cr-ZGO, 3Cr-ZGO, 5Cr-ZGO, and 7Cr-ZGO, respectively. (f) EDS of 5Sc-ZGO.

The microstructures and relative density of Sc-ZGO ceramics sintered at 1350ºC for 2 hours are shown in Fig. 1(a-e), and Fig. 1(f) shown the EDS spectrum of 5Sc-ZGO. As the Sc modification content increasing, the average size varied slightly, however, the relative density is different. It first increased with increasing Sc^{3+} content from 0.1-0.7mol% and achieved the highest density at 5Sc-ZGO, then decreased at 7Sc-ZGO. Thus, Sc^{3+} modification also improves the densification of $ZnGa_2O_4$. A relative density of 97% is reachable with Sc^{3+} content ranging from 0-0.7mol%.

Crystal structure and cation distribution

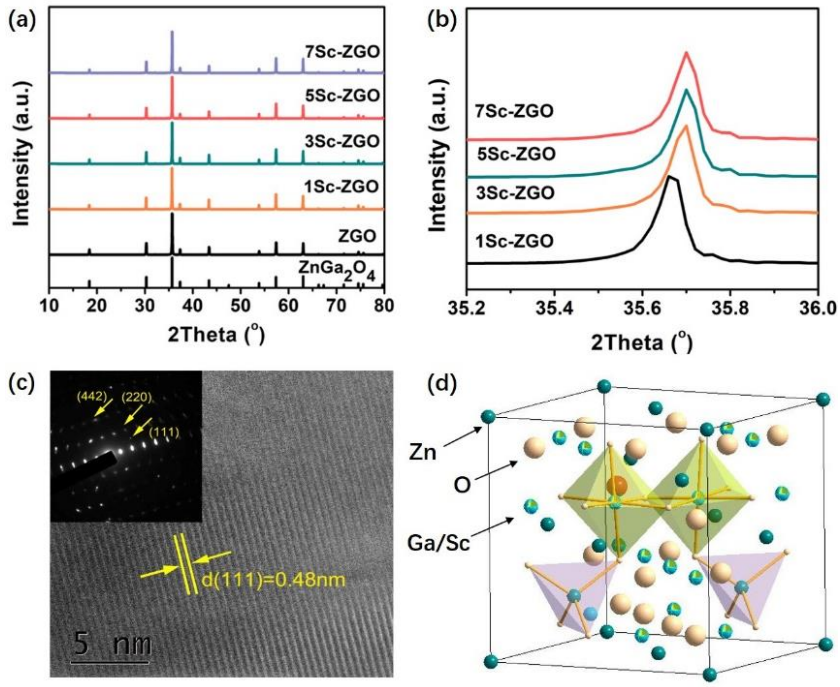

Fig. 2 (a) XRD pattern of Sc-ZGO sintered at 1350°C for 2 h, (b) enlarged XRD patterns at 2θ= 35.2-36.0, and (c) TEM image of 5Sc-ZGO. (d) Crystal structure of Sc-ZGO.

The XRD patterns of Sc-ZGO ceramics with Sc^{3+} modification content ranging from 0-0.7mol% are shown in Fig. 2(a). Fig. 2(b) is the enlarged XRD patterns at 2θ= 35.2-36.0. All the samples can be indexed as pure spinel structured $ZnGa_2O_4$ (JCPDS card no. 86-0413). Due to the Sc modification, the main diffraction peak (~35.6°) shifts to higher diffraction degree which reveals lattice contraction in the Sc-ZGO crystals.

Fig. 2(c) shows an exemplar HRTEM image together with the SAED pattern in the inset, taken from 5Sc-ZGO. The lattice spacing is 0.48 nm which corresponds to the spacing between the (111) planes of spinel structured $ZnGa_2O_4$. SAED pattern can provide further insight into the ceramic crystal structure. It can be indexed as a spinel structure with Face-Centered Cubic symmetry and a zone axis of $[1\bar{1}0]$. The sharp diffraction spots in the SAED pattern, indicating Sc-ZGO possesses good crystallinity.

Confirming by previous XRD analysis, the higher Sc^{3+} concentration means the larger lattice contraction. This indicates that Sc-ZGO is a solid solution in the range from 0.1-0.7mol% of Sc^{3+}. Therefore, Sc^{3+} entered into $ZnGa_2O_4$ structure which exhibited in Fig. 2(d).

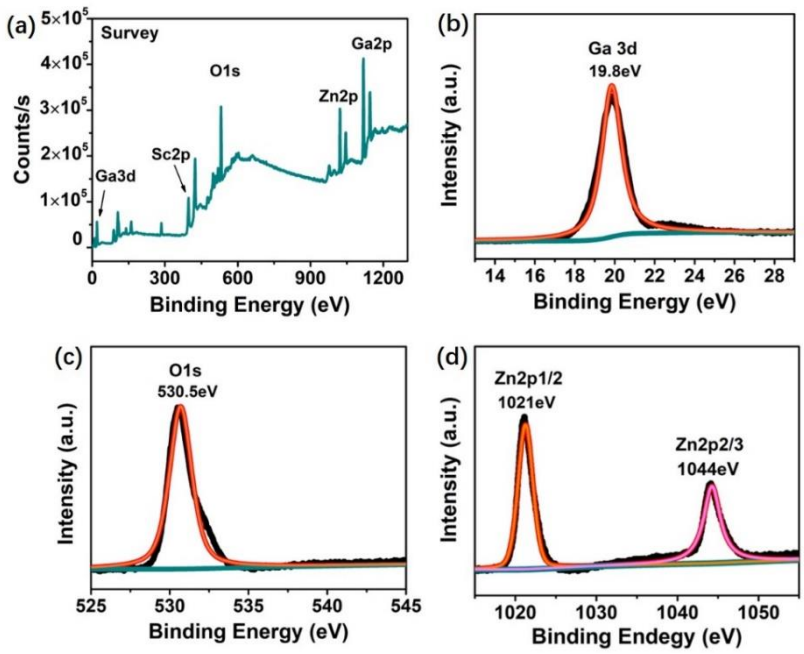

Fig. 3 XPS spectra of the middle part of $ZnGa_2O_4$ sintered at 1350℃ for 2 h, (a) full spectra, (b) Ga, (c) O, (d) Zn.

XPS spectrum of 5Sc-ZGO sintered at 1350℃ for 2 h are shown in Fig. 3. These 5 peaks, Ga 3d, Sc 2p, O 1s, Zn 2p and Ga 2p peaks can be clearly seen in the full XPS spectrum in Fig. 3(a). And the reflection peaks at 19.8eV, 530.5eV, and 1044eV binding energy in Fig. 3(c-d), are corresponding to Ga 3d, O 1s, and Zn 2p, respectively. These means Sc existed as trivalent state in Sc-ZGO, and Sc^{3+} modification didn't affect bond valence of $ZnGa_2O_4$.

Microwave dielectric properties

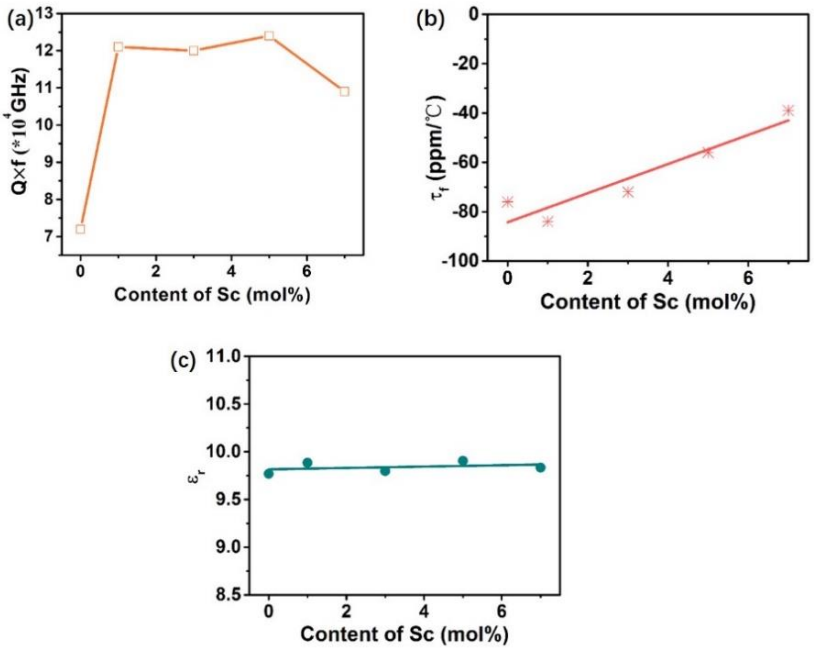

Fig. 4 Effect of Sc^{3+} modification on the microwave dielectric properties of $ZnGa_2O_4$ sintered at 1350°C for 2 h. (a) quality factor ($Q\times f$) at various sintering temperatures, (b) temperature

coefficient at resonant frequency (τ_f), and (c) dielectric constant (ε_r).

The microwave dielectric properties of Sc-ZGO sintered at 1350°C for 2 h, have been investigated and the results are shown in Fig. 4. As is shown in Fig. 4(a), the $Q\times f$ values of Sc-ZGO are strongly depend on Sc^{3+}modification. It reaches the maximum value of 124,147 GHz at 5Sc-ZGO, and then decreased with Sc^{3+} modification. According to our previous study, the $Q\times f$ value of Sc-ZGO increased by almost 1.45 times compared with unmodified $ZnGa_2O_4$. Therefore, Sc^{3+} modification is an effective way to improve $Q\times f$ values of $ZnGa_2O_4$. As already shown in Fig. 1(a), the relative density of Sc-ZGO is increased with Sc^{3+} modification. It is reasonable to note that the $Q\times f$ values are higher for those ceramics with Sc^{3+} content range from 0.1-0.5 mol%, since higher density always benefits $Q\times f$. Fig. 4(b) displays τ_f value of Sc-ZGO sintered at 1350°C for 2 h. The τ_f is -71 ppm/°C for pure ZGO, and then It increases linearly to -39 ppm/°C with Sc^{3+} modification. ε_r follows Clausius–Mossotti equation which determined by polarizabilities and molecular volume as formula (3). Due to Sc doping content is tiny (from 0.1 mol% to 0.7mol%), and the α_m of Sc^{3+} is similar with Ga^{3+}. Thus, the ε_r of Sc-ZGO keeps steady with Sc modification.

$$\varepsilon_r = [3/(1-b\alpha_m/V_m)]-2 \quad (3)$$

FT-IR and Raman analysis on the spinel structure

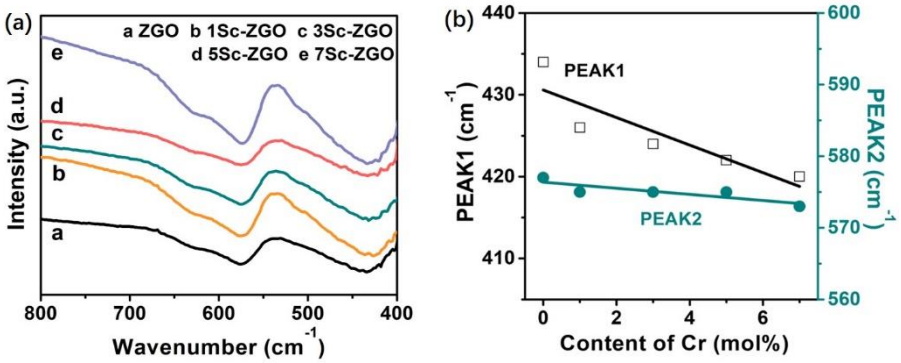

Fig. 5 (a) FT-IR spectra of Sc-ZGO, (b) the FT-IR peak positions and dielectric constant (ε_r) of the Cr-ZGO ceramics as a function of Sc content, sintered at 1350°C for 2 h.

FT-IR spectra of Sc-ZGO sintered at 1350°C for 2 h is exhibited in Fig. 5(a). Two absorption bands: 420 cm^{-1} (labeled as PEAK1) and 570 cm^{-1} (labeled as PEAK2) were observed. Both PEAK1 and PEAK2 are belongs to T_{1u} IR-active mode. These two T_{1u} modes are induced predominantly by the vibrations of the octahedral site [30]. Hence, FT-IR spectrum can reflect the octahedral distortion in Sc-ZGO crystal structure. The absorption bands shift to lower wave number with Sc^{3+} content increasing which can be observed in Fig. 5(b), both for PEAK1 (from 434cm^{-1} to 420cm^{-1}) and PEAK2 (from 577cm^{-1} to 573cm^{-1}). These two FT-IR peaks shift was sensitive to Sc^{3+} and shown linear correlation with Sc^{3+} concentration, which means FT-IR shift were caused by Sc modification. Cause FT-IR absorption demonstrate bond vibration, the linear correlation between Sc^{3+} modification and FT-IR shift reflects that Sc^{3+} modification effectively influence ZGO bond vibration.

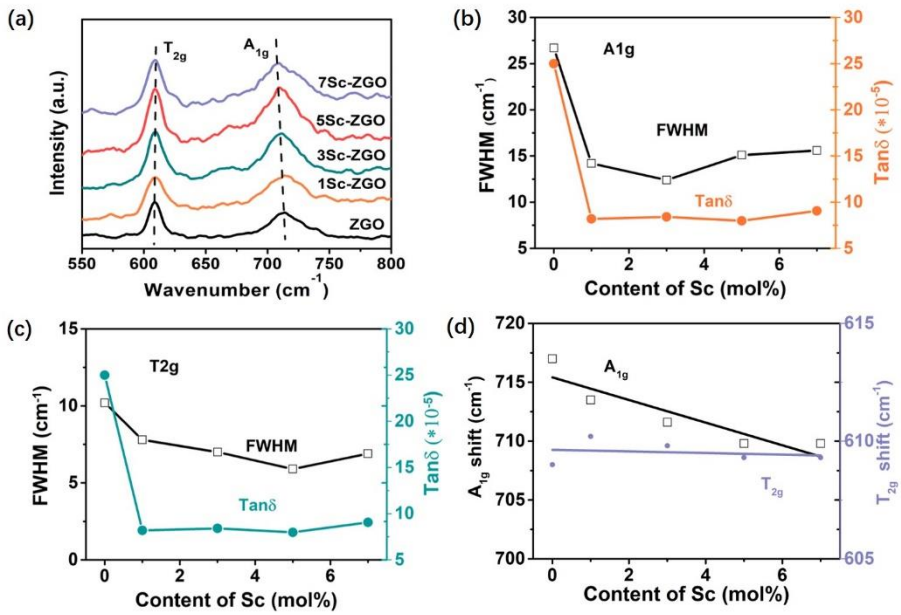

Fig. 6 (a)Raman spectra of Cr^{3+} modified $ZnGa_2O_4$, (b) FWHM value of the A_{1g} mode and dielectric loss (tanδ), (c) FWHM value of the T_{2g} mode and dielectric loss (tanδ), (d) A_{1g} shift and T_{2g} shift of Sc-ZGO ceramics as a function of Sc^{3+} concentration, sintered at 1350ºC for 2 h.

Fig.6(a) exhibits the Raman spectrum of Sc-ZGO. Two peaks: T_{2g} phonon mode at ~607 cm^{-1} and A_{1g} phonon mode at ~712 cm^{-1} can be clearly seen which is consistent with $ZnGa_2O_4$ Raman characterization reported by Wiglusz [31]. The two T_{2g} and A_{1g} phonon modes in Fig.6(a) are the first order Raman modes. T_{2g} phonon mode is the breathing mode of the octahedral site, and A_{1g} phonon mode is the stretching vibration in the tetrahedral site, respectively.

For perovskite materials, the full width at half maxima (FWHM) of Raman phonon mode is indicative of the short-range cation ordering and can be used to explain tanδ variety [22-35]. Perovskite materials with higher short-range cation ordering degree usually possess lower Raman FWHM and higher $Q\times f$. As perovskite and spinel materials have a similar crystal structure, it can be supposed that the tanδ of spinel structured materials has a correlation with Raman FWHM. The FWHM of the A_{1g}, T_{2g} phonon modes and tanδ of Sc-ZGO have been compiled in Fig. 6(b-c). The Raman shifts of the A_{1g} and T_{2g} phonon modes, and ε_r with increasing Sc^{3+} modification is compiled in Fig. 6(d). As FT-IR shift discussed above, these two Raman modes shift was sensitive to Sc^{3+} and shown linear relation with Sc^{3+} content, which means Raman modes shift was caused by Sc^{3+} modification. Cause Raman modes also demonstrate bond vibration, and have complementary relationship with FT-IR modes. The linear correlation between Sc^{3+} modification and Raman modes shift reflects that Sc^{3+} modification effectively influence ZGO bond vibration.

Conclusions

Sc-modified $ZnGa_2O_4$ with excellent microwave dielectric properties have been successfully synthesized. Due to the tiny modification concentration and ionic polarization, with the increase Sc^{3+} content, ε_r of Sc-ZGO ceramics keeps steady. The $Q\times f$ value of Sc-ZGO ceramics ramp up to a maximum at 0.5mol% Sc^{3+} modification

and then ramp down continuously. In the Sc^{3+} content range from 0 to 0.5mol% it increased from 83,000 GHz to 124,147 GHz and then decreased to 109,366 GHz. The τ_f value of Sc-ZGO increased linearly with Sc^{3+} concentration from -71ppm/°C to -39 ppm/°C. Great microwave dielectric performance was achieved in 5Sc-ZGO spinel ceramics sintered at 1350°C for 2h: ε_r = 9.9, $Q\times f$ = 124,147 GHz, tanδ = 7.98×10^{-5}, and τ_f = -56 ppm/°C. The higher densification do benefit the $Q\times f$. However, Raman and FT-IR analysis on Sc^{3+} modified $ZnGa_2O_4$ further elucidated that when the relative density is much the same, the short-range cation ordering degree is the dominant factor to higher $Q\times f$. The Raman shift of A_{1g} and T_{2g} phonon modes and FT-IR shift further confirm bond vibration induced by Sc^{3+} modification. The tanδ was found to follow closely with the FWHM of A_{1g} and T_{2g} modes which represents the short-range cation ordering degree. The maximum $Q\times f$ value for 5Cr-ZGO can be attributed to the highest short-range cation ordering degree and highest density, while the decrease of $Q\times f$ of 7Sc-ZGO can be ascribed to the decrease of short-range cation ordering degree and lower density.

Conflicts of interest

There are no conflicts to declare.

Acknowledgement

This work was supported in part by the open research fund of the National and Local Joint Engineering Laboratory of RF Integration and Micro-Assembly Technology (Grant Nos. KFJJ20180205), the NUPTSF (Grant No. NY218113, No. NY219077), the Opening Project of the State Key Laboratory of High-Performance Ceramics and Superfine Microstructure (Project no. SKL201 309SIC), and the open research program of state key lab. of millimeter waves in southeast university(K201928).

References

[1] H. Ji, X. Hou, M.S. Molokeev, J. Ueda, S. Tanabe, M.G. Brik, Ultrabroadband red luminescence of Mn^{4+} in $MgAl_2O_4$ peaking at 651 nm, Dalton Transactions, 49(2020): 5711-5721.

[2] T.A. Safeera, J. Johny, S. Shaji, Y.T. Nien, E.I. Anila, Impact of activator incorporation on red emitting rods of $ZnGa_2O_4$:Cr^{3+} phosphor, Materials science & engineering, 94(2019):1037-1043.

[3] A. Saad, H. Shen, Z. Cheng, Q. Ju, M. Yang, Three-Dimensional Mesoporous Phosphide-Spinel Oxide Heterojunctions with Dual Function as Catalysts for Overall Water Splitting, ACS Applied Energy Materials, 3(2020):1684-1693.

[4] F. Gao, C. Chu, W. Zhu, X. Tang, H.Yi, High-efficiency catalytic oxidation of nitric oxide over spherical Mn Co spinel catalyst at low temperature, Applied Surface Science, 479(2019):548-556.

[5] D.H. Kim, S. Ning, C.A. Ross, Self-assembled multiferroic perovskite–spinel nanocomposite thin films: epitaxial growth, templating and integration on silicon, Journal of Materials Chemistry C, 7(2019): 9128-9148.

[6] A. Sahu, R. Chaurashiya, K. Hiremath, A. Dixit, Nanostructured zinc titanate wide

band gap semiconductor as a photoelectrode material for quantum dot sensitized solar cells, Solar Energy, 163(2018):338-346.
[7] Z. Wei, G. He, W. Hu, Z. Feng, K. Jin, Anomalies of upper critical field in the spinel superconductor $LiTi_2O_4$-delta, Physical Review B, 100(2019), 184509.
[8] K. Jin, G. He, X. Zhang, S. Maruyama, S. Yasui, R. Suchoski, Anomalous magnetoresistance in the spinel superconductor $LiTi_2O_4$, Nature Communications, 6(2015),7183.
[9] W.J Bian, X.C. Lu, Y. Wang, H.K Zhu, T. Chen, S.W. Ta, Q.T. Zhang, Correlations between structure and microwave dielectric properties of Co doped $MgMoO_4$ ceramics, Ceramics International, 46 (2020): 22024-22029.
[10] W.J. Bian, X.C. Lu, Y.Y. Li, C.F. Min, H.K. Zhu, Z.X. Fu, Q.T. Zhang, Influence of Nd doping on microwave dielectric properties of $SrTiO_3$ ceramics, Journal of Materials Science: Materials in Electronics, 29 (2018): 2743-2747.
[11] A. Kan, T. Moriyama, S. Takahashi, H. Ogawa, Cation distributions and microwave dielectric properties of spinel-structured $MgGa_2O_4$ ceramics, Japanese Journal of applied physics, 52(2013), 09KH01.
[12] S. Takahashi, A. Kan, H. Ogawa, Microwave dielectric properties and crystal structures of spinel structured $MgAl_2O_4$ ceramics synthesized by a molten-salt method, Journal European Ceramics Society, 37(2016): 1001-1006.
[13] Y.C. Chen, H.M. You, K.C. Chang, Influence of Li_2WO_4, aid and sintering temperature on microstructures and microwave dielectric properties of Zn_2SnO_4 ceramics, Ceramics International, 41(2014): 5257-5262.
[14] R.Z. Zuo, J. Zhang, J. Song, Y.D. Xu, Liquid-phase sintering, microstructural evolution and microwave dielectric properties of $Li_2Mg_3SnO_6$-LiF ceramics, Journal of American Ceramics Society, 101(2017), 569-576.
[15] X.L Jing, X.L Tang, W.H. Tang, Y.L. Jing, H. Su, Effects of Zn^{2+} substitution on the sintering behavior and dielectric properties of $Li_2Mg_{1-x}Zn_xSiO_4$ ceramics, Applied Physics A, 125(2019), 415.
[16] H.W. Chen, H. Su, H.W. Zhang, T.C. Zhou, B.W. Zhang, J.F. Zhang, X.L. Tang, Low-temperature sintering and microwave dielectric properties of $(Zn_{1-x}Co_x)_2SiO_4$ ceramics, Ceramics International, 40(2014): 14655-14659.
[17] X.K. Lan, J. Li, Z.T. Zou, M.K. Xie, W. Lei, Improved sinterability and microwave dielectric properties of $[Zn_{0.5}Ti_{0.5}]^{3+}$ doped $ZnAl_2O_4$ spinel solid solution, Journal of American Ceramics Society, 102(2019): 5952-5957.
[18] S. Takahashi, A. Kan, H. Ogawa, Microwave dielectric properties and crystal structures of $Mg_{0.7}Al_{2.2}O_4$ and $Mg_{0.4}Al_{2.4}O_4$ ceramics with defect structures, Journal of American Ceramics Society, 100(2017): 3497-3504.
[19]X.C. Lu, W.J. Bian, B. Quan, Z.F. Wang, H.K. Zhu, Q.T. Zhang, Compositional tailoring effect on $ZnGa_2O_4$-TiO_2 ceramics for tunable microwave dielectric properties, Journal of Alloys and Compounds, 792(2019): 742-749.
[20]X.C. Lu, W.J. Bian, C.F. Min, Z.X. Fu, Q.T. Zhang, H.K. Zhu, Cation distribution of high-performance Mn-substituted $ZnGa_2O_4$ microwave dielectric ceramics, Ceramics International, 44(2018): 10028-10034.
[21] X.C. Lu, Z.H. Du, B. Quan, W.J. Bian, H.K. Zhu, Q.T. Zhang, Structural

dependence of microwave dielectric properties of Cr^{3+}-substituted $ZnGa_2O_4$ spinel ceramics: crystal distortion and vibration modes study, Journal of Materials Chemistry C, 7(2019): 8261-8268.
[22] X.C. Lu, W.J. Bian, Y.Y. Li, H.K. Zhu, Z.X. Fu, Q.T. Zhang, Influence of inverse spinel structured $CuGa_2O_4$ on microwave dielectric properties of normal spinel $ZnGa_2O_4$ ceramics, Journal of the American Ceramic Society, 101(2018): 1646-1654.
[23] X.C. Lu, W.J. Bian, Y.Y. Li, H.K. Zhu, Z.X. Fu, Q.T. Zhang, Cation distributions and microwave dielectric properties of Cu-substituted $ZnGa_2O_4$ spinel ceramics, Ceramics International, 43(2017): 13839-13844.
[24] S. Zhang, H. Sahin, E. Torun, F. Peeters, D. Martien, T. Dapron, N. Dilley, N. Newman, Fundamental mechanisms responsible for the temperature coefficient of resonant frequency in microwave dielectric ceramics, Journal of American Ceramics Society, 100(2017): 1508-1516.
[25] M.T. Sebastian, Dielectric materials for wireless communication, Journal Materials Chemistry, 11(2010): 54-62.
[26] N. Udomkan, P. Limsuwan, T. Tunkasiri, Effect of rare-earth (RE = La, Nd, Ce and Gd) doping on the piezoelectric of PZT(52:48) ceramics, International Journal of Modern Physics B, 21(2009): 4549-4559.
[27] J. Takahashi, T. Ikegami, K. Kageyama, Occurrence of Dielectric 1:1:4 Compound in the Ternary System BaO-Ln_2O_3-TiO_2 (Ln = La, Nd, and Sm): II, Reexamination of Formation of Isostructural Ternary Compounds in Identical Systems, Journal of the American Ceramic Society, 74(1991): 1868-1872 .
[28] Hisakazu Takahashi, Yoko Baba, Kenichi Ezaki, Microwave Dielectric Properties and Crystal Structure of CaO-Li_2O-$(1-x)Sm_2O_3$-xLn_2O_3-TiO_2 (Ln: lanthanide) Ceramics System, Japanese Journal of Applied Physics, 9B(1996): 5069-5073.
[29] X.C. Fan, X.M. Chen, X.Q. Liu, Complex-permittivity measurement on high-Q materials via combined numerical approaches, IEEE Transactions on Microwave Theory & Techniques, 53(2005): 3130-3134.
[30] S.P. Wu, J.J. Xue, R. Wang, J.H. Li, Synthesis, characterization and microwave dielectric properties of spinel $MgGa_2O_4$ ceramic materials, Journal of Alloys and Compounds, 585(2014): 542-548.
[31] R.J. Wiglusz, A. Watras, M. Malecka, P.J. Deren, R. Pazik, Structure Evolution and Up-Conversion Studies of ZnX_2O_4:Er^{3+}/Yb^{3+}(X = Al^{3+}, Ga^{3+}, In^{3+}) Nanoparticles, European Journal of Inorganic Chemistry, 6(2014), 1090-1101.
[32] M.S. Fu, X.Q. Liu, X.M. Chen, Erratum: giant dielectric response in two-dimensional charge-ordered nickelate ceramics, Journal of Applied Physics, 105(2008), 129902.
[33] C.L. Diao, F. Shi, Correlation among Dielectric Properties, Vibrational Modes, and Crystal Structures in $Ba[Sn_xZn_{(1-x)/3}Nb_{2(1-x)/3}]O_3$ Solid Solutions, Journal of Physical Chemistry C, 116(2012):6852-6858.
[34] F. Shi, H. Dong, Correlation of phonon characteristics and crystal structures of $Ba[Zn_{1/3}(Nb_{1-x}Ta_x)_{2/3}]O_3$ solid solutions, Journal of Applied Physics, 111(2012): 1-5.
[35] F. Shi, H. Dong, Correlation between vibrational modes and structural characteristics of $Ba[(Zn_{1-x}Mg_x)_{1/3}Ta_{2/3}]O_3$ solid solutions, CrystEngComm, 14(2012):

3373-3379.

Figures

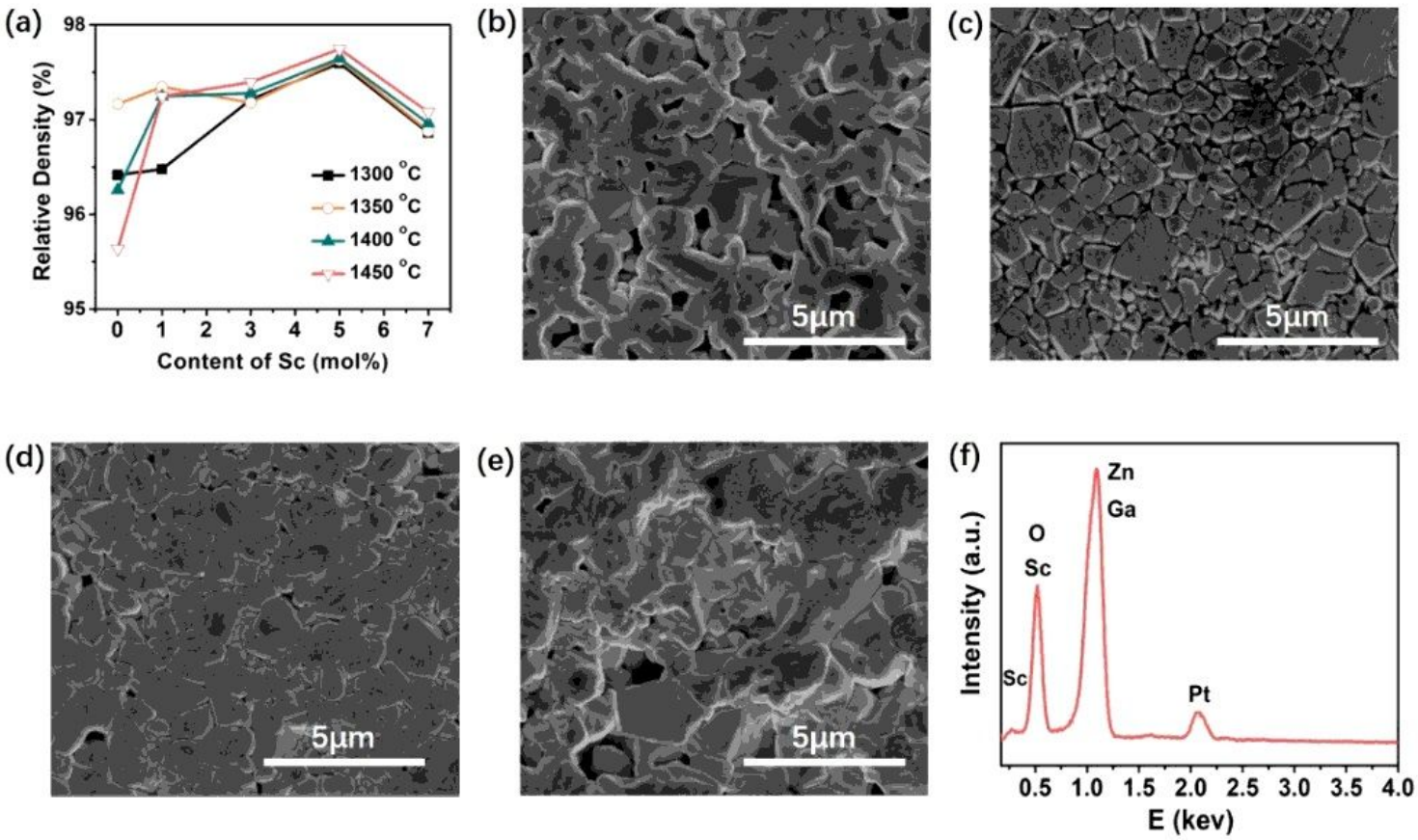

Figure 1

(a) Relative density of Sc-ZGO, SEM images of Sc-ZGO sintered at 1350 oC for 2 h and (b-e) are 1Cr-ZGO, 3Cr-ZGO, 5Cr-ZGO, and 7Cr-ZGO, respectively. (f) EDS of 5Sc-ZGO.

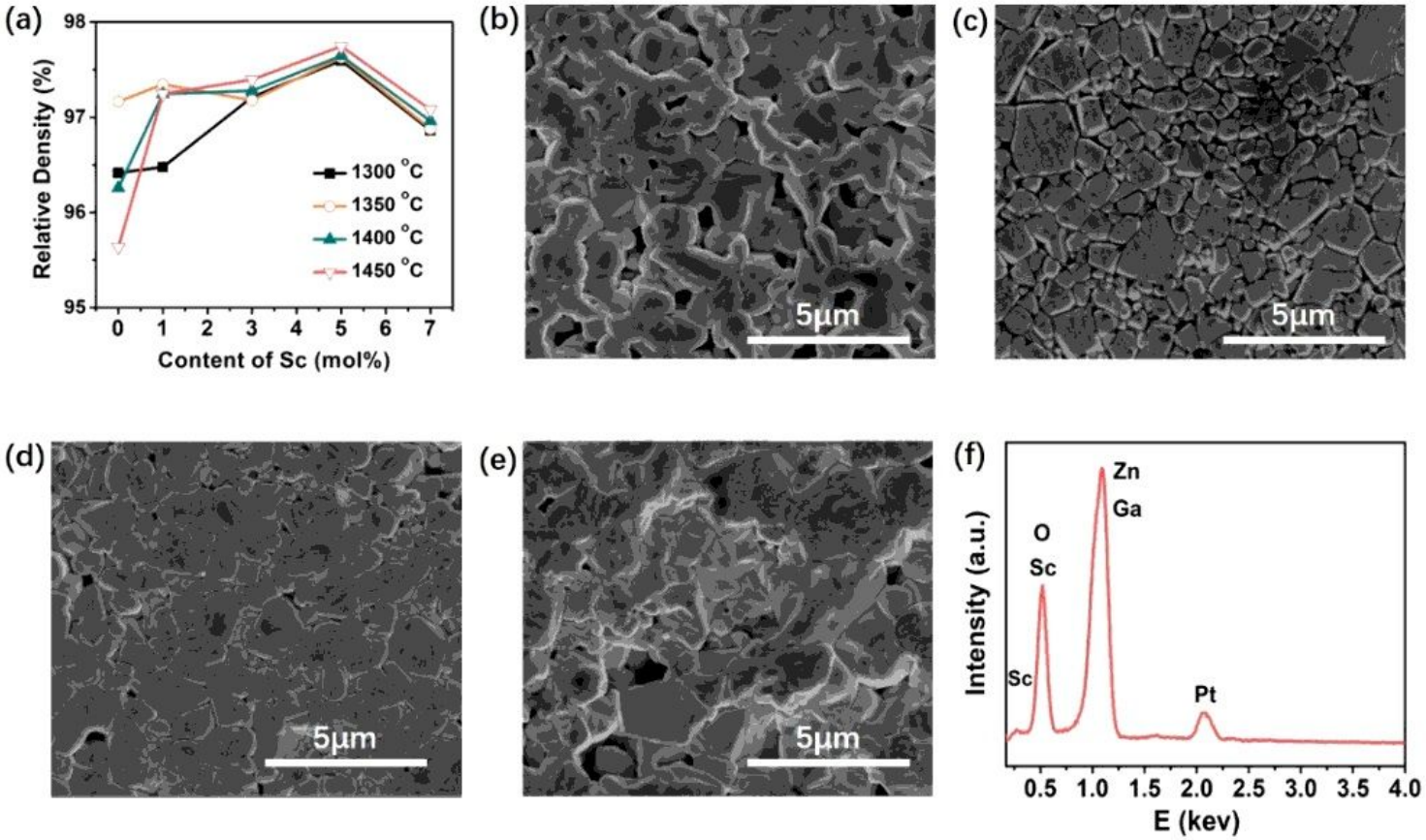

Figure 1

(a) Relative density of Sc-ZGO, SEM images of Sc-ZGO sintered at 1350 oC for 2 h and (b-e) are 1Cr-ZGO, 3Cr-ZGO, 5Cr-ZGO, and 7Cr-ZGO, respectively. (f) EDS of 5Sc-ZGO.

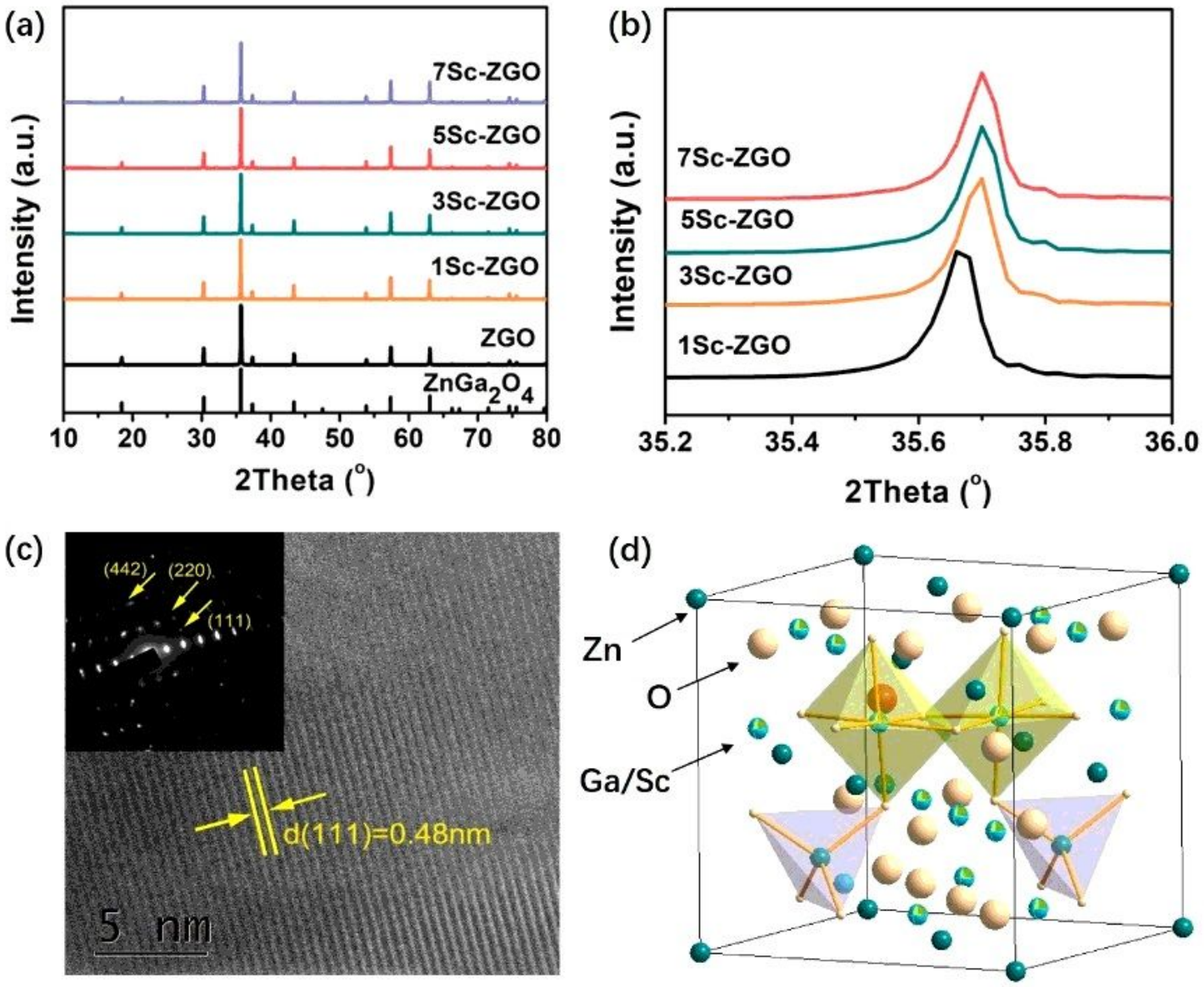

Figure 2

(a) XRD pattern of Sc-ZGO sintered at 1350oC for 2 h, (b) enlarged XRD patterns at 2θ= 35.2-36.0, and (c) TEM image of 5Sc-ZGO. (d) Crystal structure of Sc-ZGO.

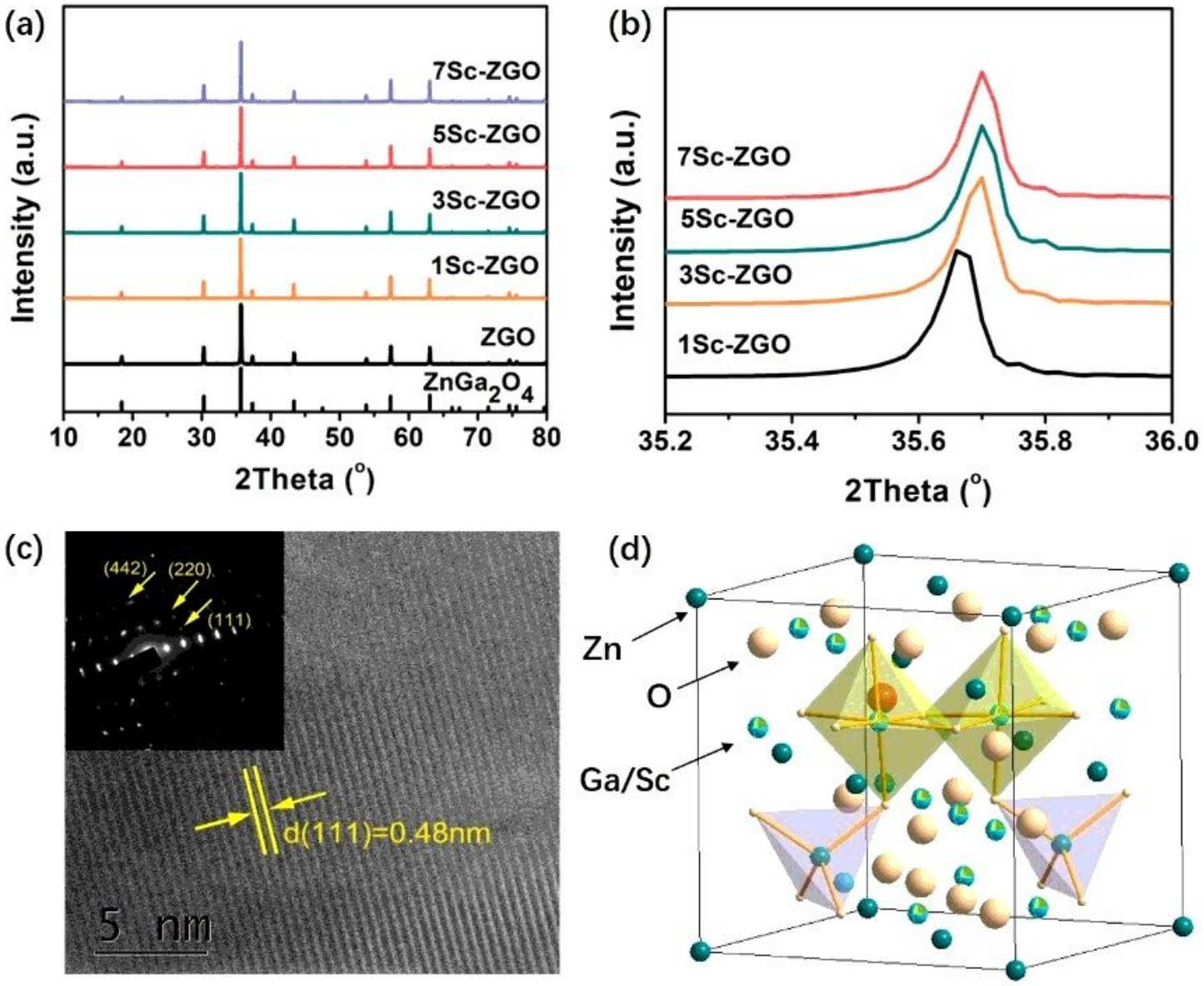

Figure 2

(a) XRD pattern of Sc-ZGO sintered at 1350oC for 2 h, (b) enlarged XRD patterns at 2θ= 35.2-36.0, and (c) TEM image of 5Sc-ZGO. (d) Crystal structure of Sc-ZGO.

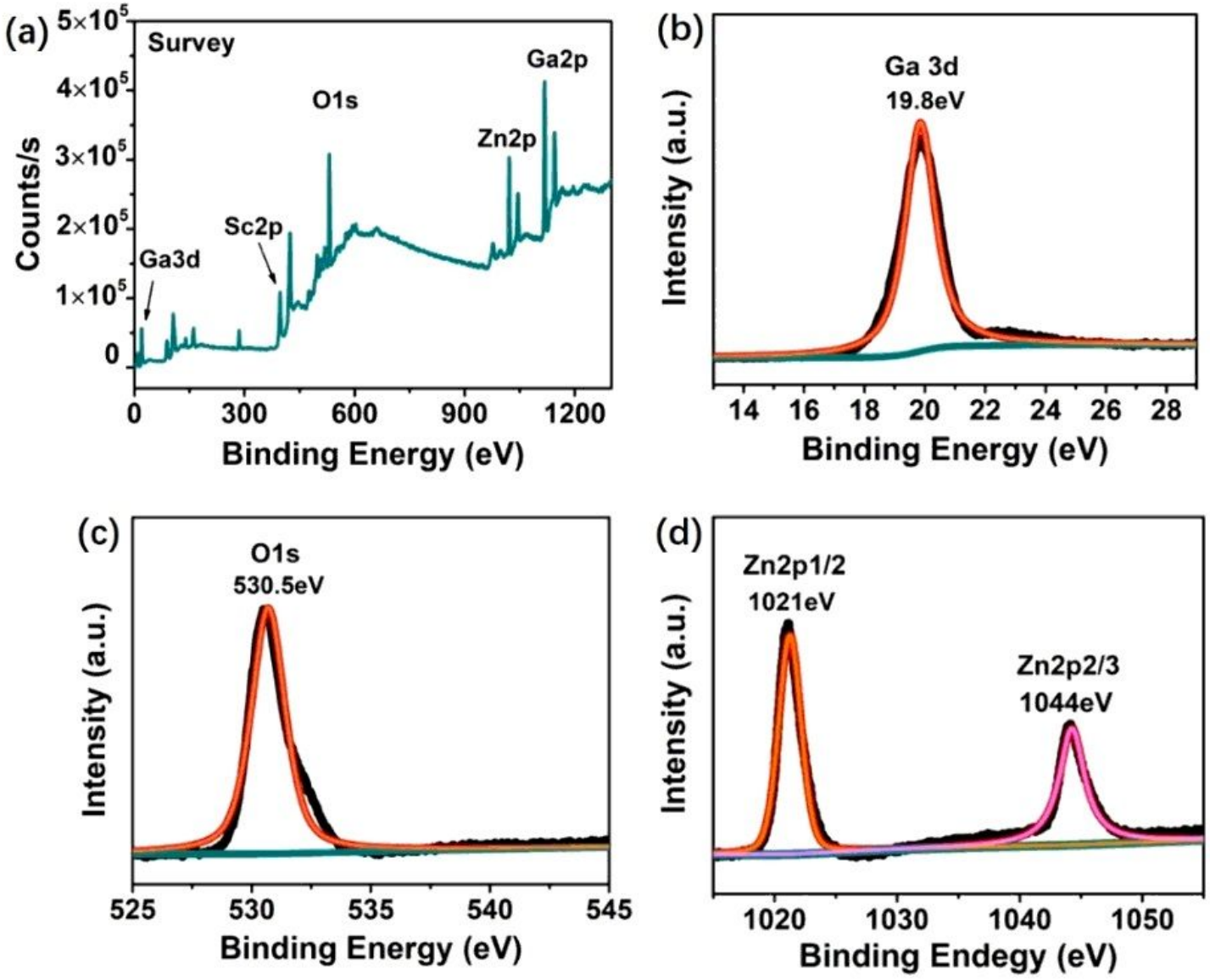

Figure 3

XPS spectra of the middle part of ZnGa2O4 sintered at 1350□ for 2 h, (a) full spectra, (b) Ga, (c) O, (d) Zn.

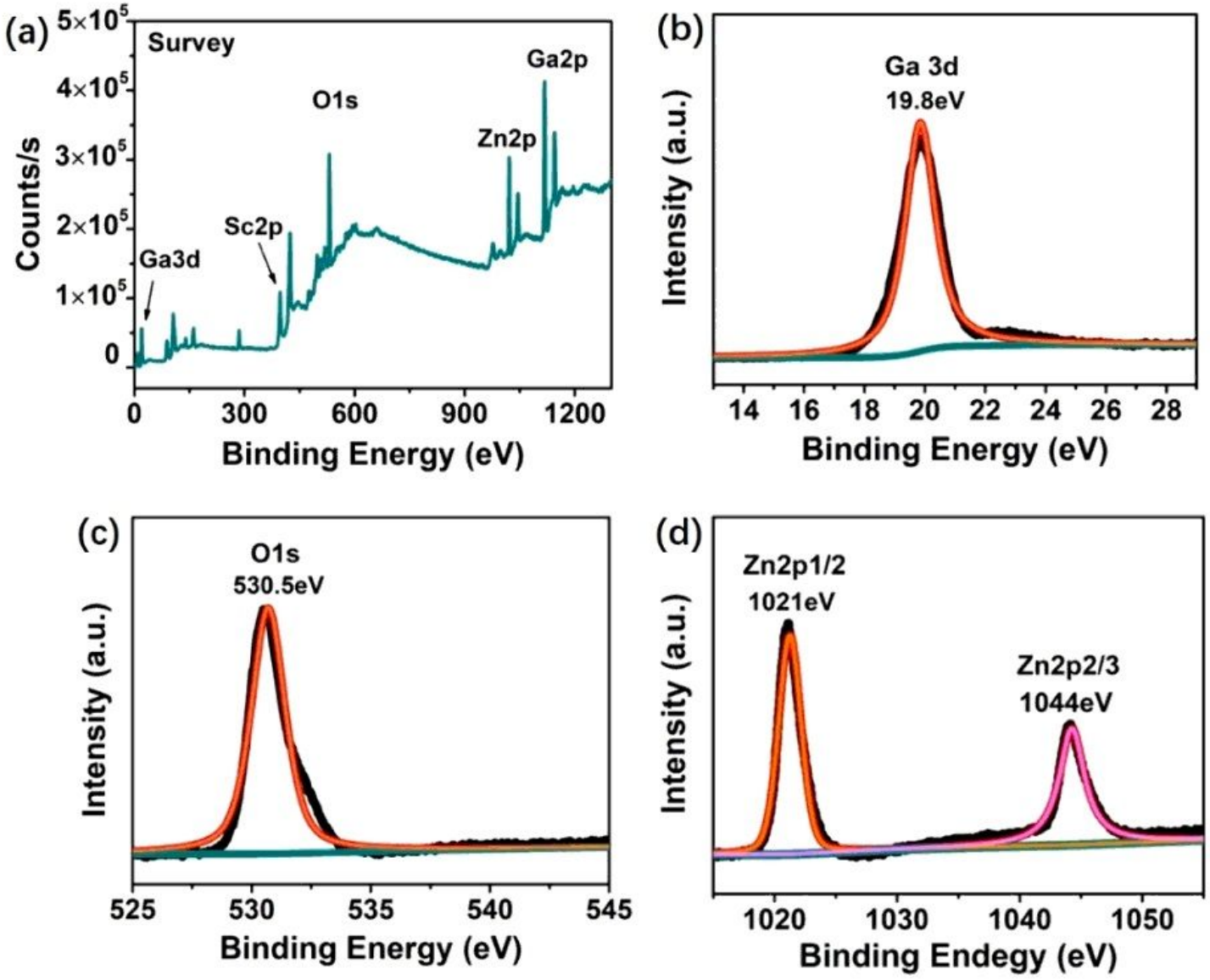

Figure 3

XPS spectra of the middle part of ZnGa2O4 sintered at 1350□ for 2 h, (a) full spectra, (b) Ga, (c) O, (d) Zn.

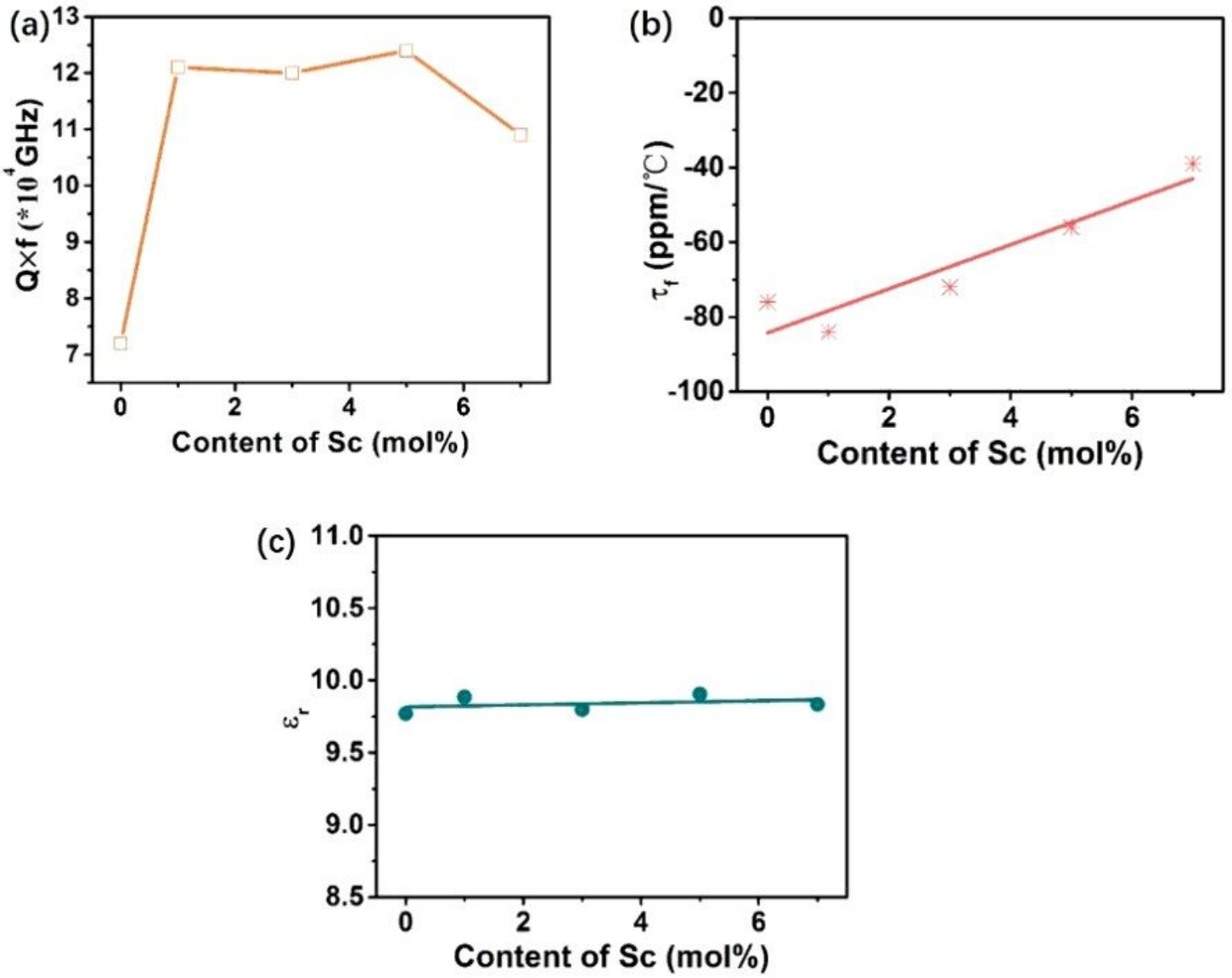

Figure 4

Effect of Sc3+ modification on the microwave dielectric properties of ZnGa2O4 sintered at 1350oC for 2 h. (a) quality factor (Q×f) at various sintering temperatures, (b) temperature coefficient at resonant frequency (τf), and (c) dielectric constant (εr).

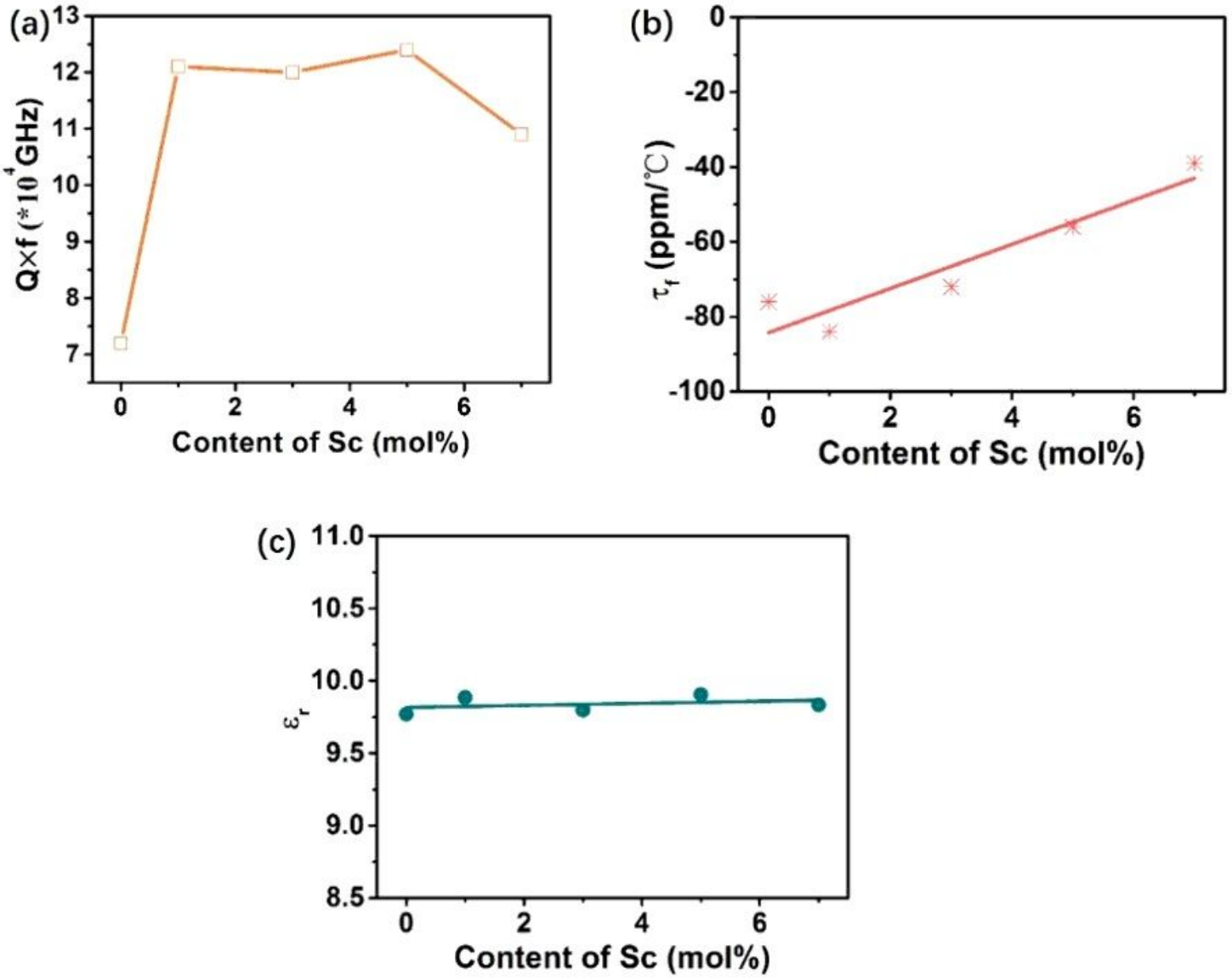

Figure 4

Effect of Sc3+ modification on the microwave dielectric properties of ZnGa2O4 sintered at 1350oC for 2 h. (a) quality factor (Q×f) at various sintering temperatures, (b) temperature coefficient at resonant frequency (τf), and (c) dielectric constant (εr).

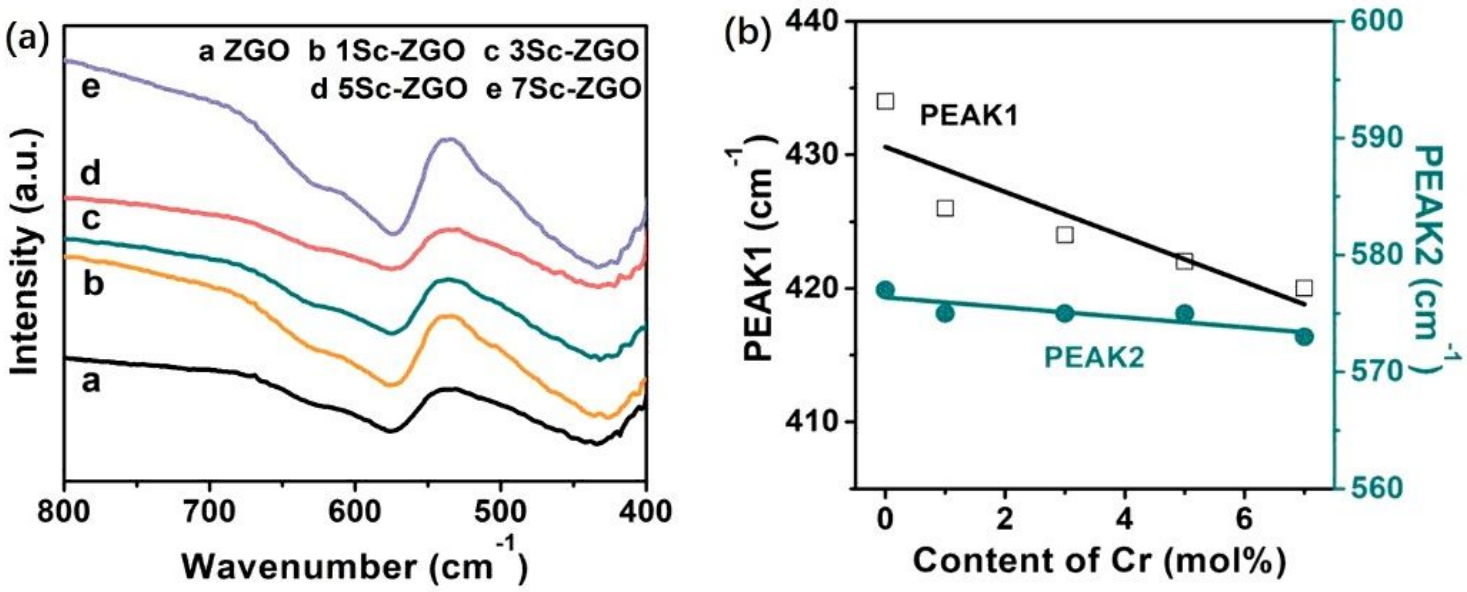

Figure 5

(a) FT-IR spectra of Sc-ZGO, (b) the FT-IR peak positions and dielectric constant (εr) of the Cr-ZGO ceramics as a function of Sc content, sintered at 1350oC for 2 h.

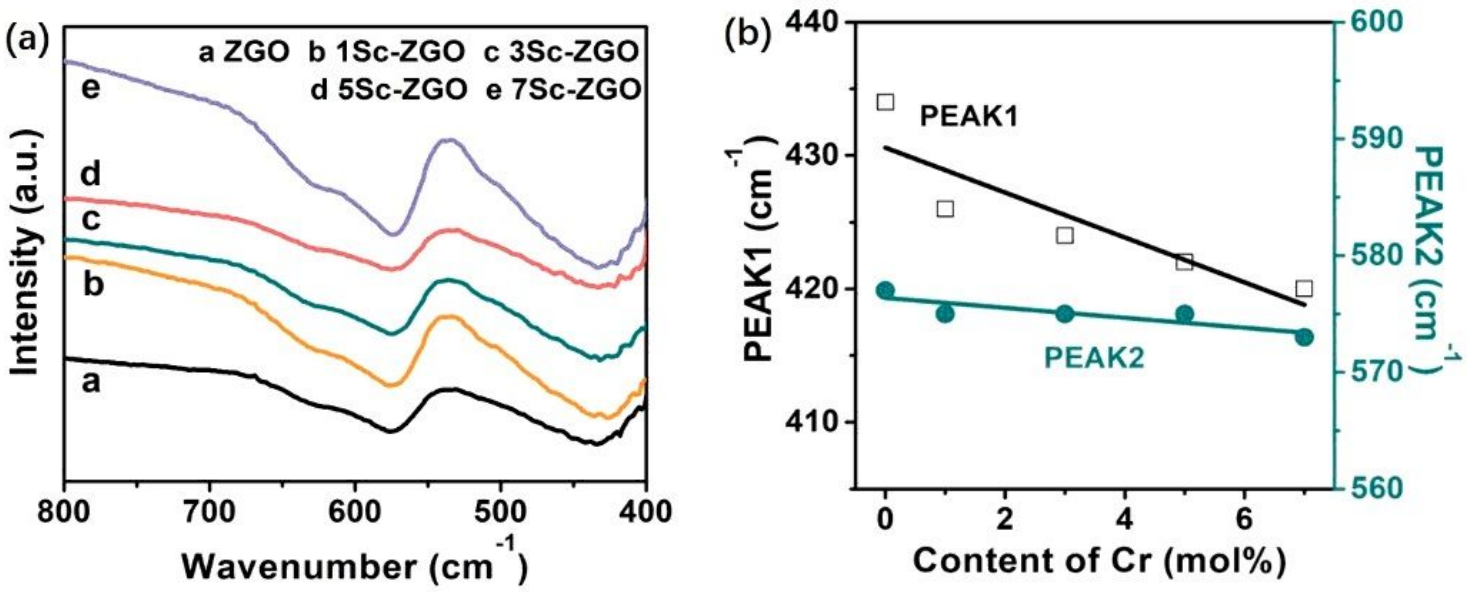

Figure 5

(a) FT-IR spectra of Sc-ZGO, (b) the FT-IR peak positions and dielectric constant (εr) of the Cr-ZGO ceramics as a function of Sc content, sintered at 1350oC for 2 h.

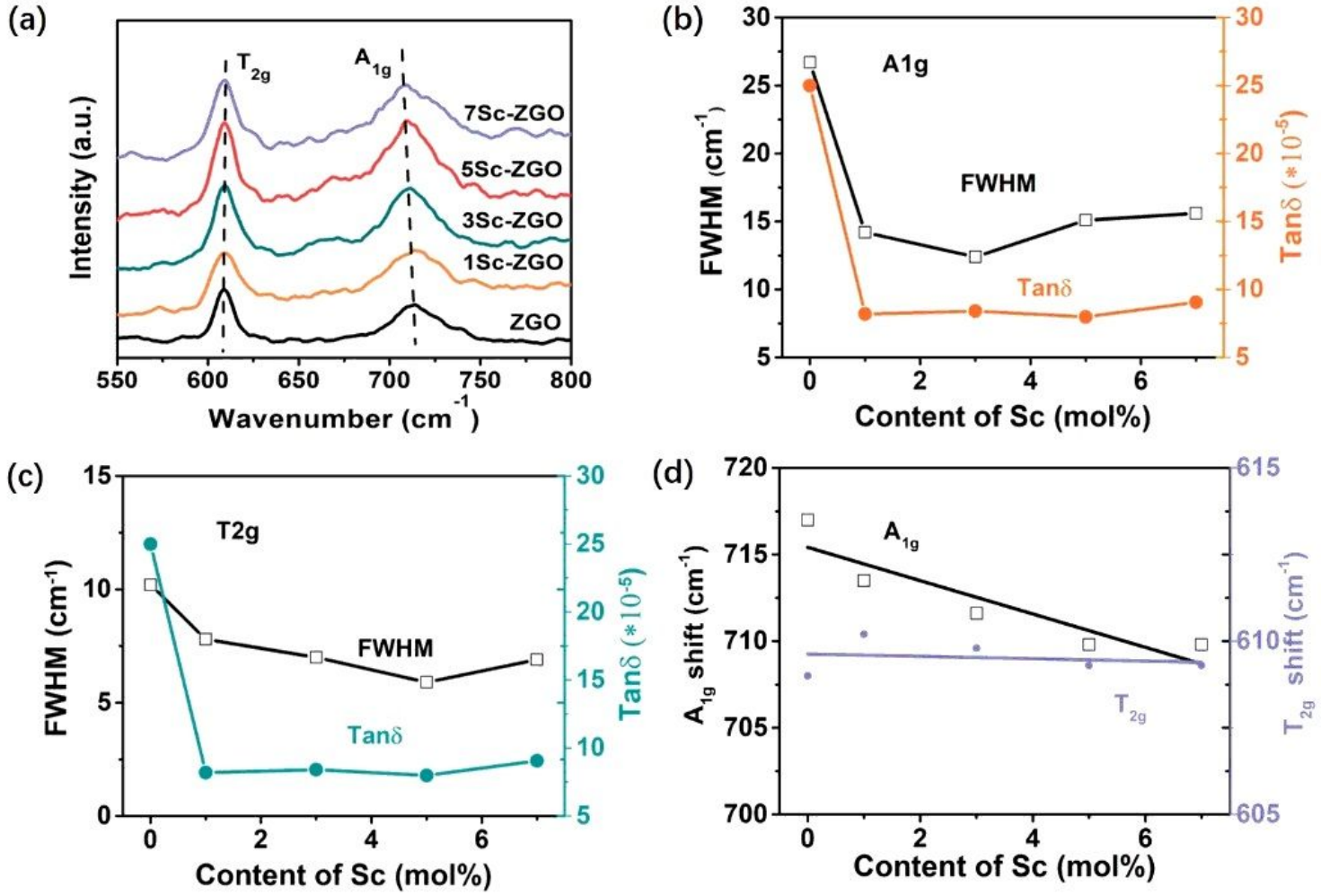

Figure 6

(a)Raman spectra of Cr3+ modified ZnGa2O4, (b) FWHM value of the A1g mode and dielectric loss (tanδ), (c) FWHM value of the T2g mode and dielectric loss (tanδ), (d) A1g shift and T2g shift of Sc-ZGO ceramics as a function of Sc3+ concentration, sintered at 1350oC for 2 h.

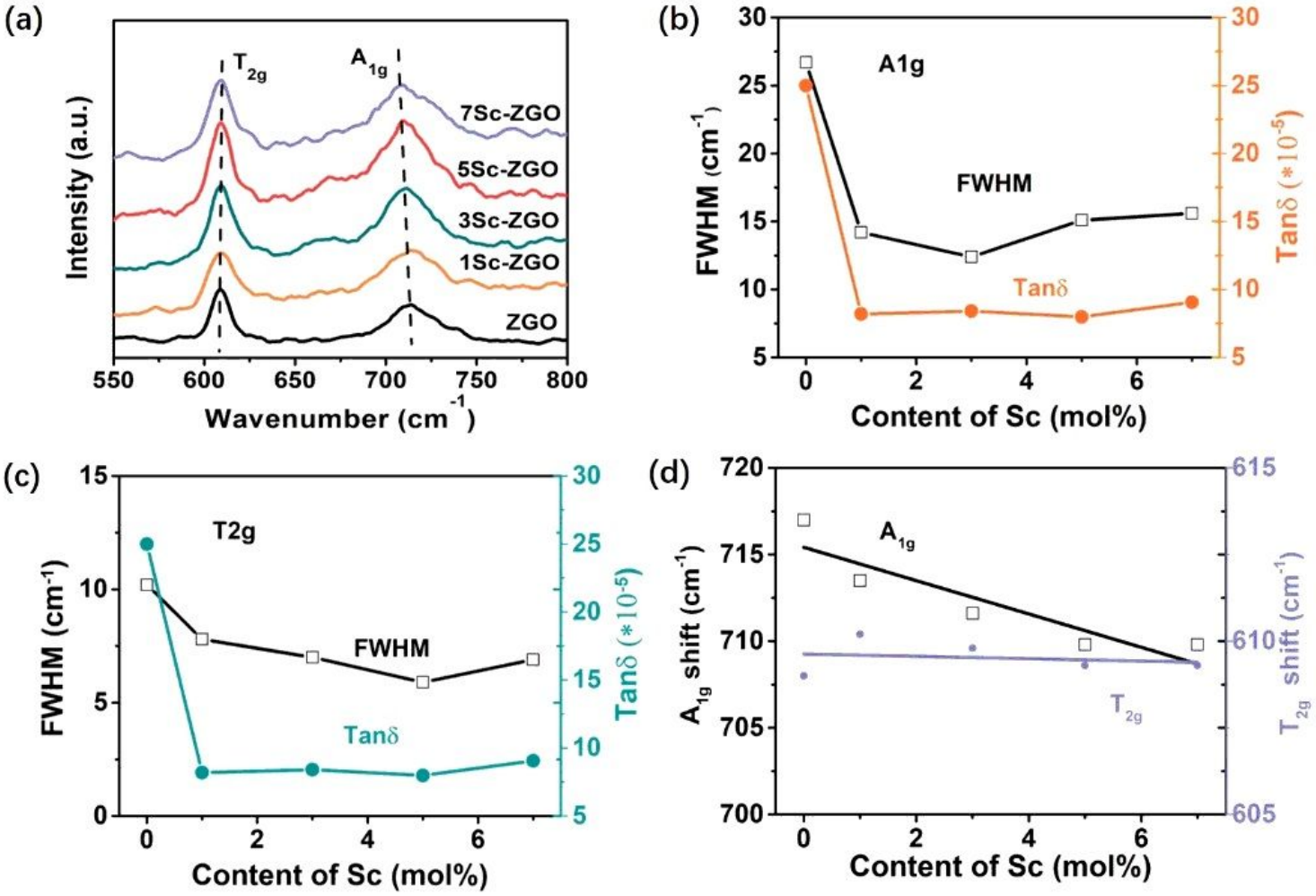

Figure 6

(a)Raman spectra of Cr3+ modified ZnGa2O4, (b) FWHM value of the A1g mode and dielectric loss (tanδ), (c) FWHM value of the T2g mode and dielectric loss (tanδ), (d) A1g shift and T2g shift of Sc-ZGO ceramics as a function of Sc3+ concentration, sintered at 1350oC for 2 h.